HHS Public Access

Author manuscript

Bone. Author manuscript; available in PMC 2024 November 01.

Published in final edited form as:

Bone. 2023 November ; 176: 116866. doi:10.1016/j.bone.2023.116866.

G-Protein Coupled Receptor 5C (GPRC5C) is Required for Osteoblast Differentiation and Responds to EZH2 Inhibition and Multiple Osteogenic Signals

Parisa Dashti[1], **Roman Thaler**[1], **John R. Hawse**[2], **M. Lizeth Galvan**[1], **Bram J van der Eerden**[3], **Andre J. van Wijnen**[3,4,*], **Amel Dudakovic**[1,2,*]

[1]Department of Orthopedic Surgery, Mayo Clinic, Rochester, MN, USA

[2]Department of Biochemistry & Molecular Biology, Mayo Clinic, Rochester, MN, USA

[3]Department of Internal Medicine, Erasmus University Medical Center, Rotterdam, the Netherlands

[4]Department of Biochemistry, University of Vermont, Burlington, VT, USA

Abstract

Osteoblast differentiation is epigenetically suppressed by the H3K27 methyltransferase EZH2, and induced by the morphogen BMP2 and transcription factor RUNX2. These factors also regulate distinct G protein coupled receptors (GPRCs; e.g., PTH1R, GPR30/GPER1). Because GPRCs transduce many physiological stimuli, we examined whether BMP2 or EZH2 inhibition (i.e., GSK126) regulates other GPRC genes in osteoblasts. RNA-seq screening of >400 mouse GPRC-related genes showed that many GPRCs are downregulated during osteogenic differentiation. The orphan receptor GPRC5C, along with a small subset of other GPRCs, is induced by BMP2 or GSK126 during Vitamin C dependent osteoblast differentiation, but not by all-trans retinoic acid. ChIP-seq analysis revealed that GSK126 reduces H3K27me3 levels at the GPRC5C gene locus in differentiating MC3T3-E1 osteoblasts, consistent with enhanced GPRC5C mRNA expression. Loss of function analyses revealed that shRNA-mediated depletion of GPRC5C decreases expression of bone markers (e.g., BGLAP and IBSP) and mineral deposition in response to BMP2 or GSK126. GPRC5C mRNA was found to be reduced in the osteopenic bones of KLF10 null mice which have compromised BMP2 signaling. GPRC5C mRNA is induced by the bone-anabolic activity of 17β-estradiol in trabecular but not cortical bone following ovariectomy. Collectively,

[*]**To whom correspondence should be addressed:** Amel Dudakovic, Ph.D., Department of Orthopedic Surgery, Mayo Clinic, Rochester, MN, United States of America, Dudakovic.Amel@mayo.edu, Andre J. van Wijnen, Ph.D., Department of Biochemistry, University of Vermont, Burlington, VT, United States of America, andre.vanwijnen@uvm.edu.

AUTHOR CONTRIBUTIONS

PD, AJvW & AD designed experiments. PD, RT, & MLG performed experimentation. PD, RT, JHR, BJvdE, AJvW & AD analyzed and interpreted the data. PD wrote the first draft with assistance of AJvW & AD. RT, JRH, MLG, and BJvdE provided comments and edits on the first draft. PD, AJvW & AD revised the paper in response to the constructive comments of the reviewers. All authors approved the final draft of the paper.

CONFLICT OF INTEREST

The authors declare that they have no conflicts of interest with the contents of this article.

these findings suggest that GPRC5C protein is a key node in a pro-osteogenic axis that is normally suppressed by EZH2-mediated H3K27me3 marks and induced during osteoblast differentiation by GSK126, BMP2, and/or 17β-estradiol. Because GPRC5C protein is an understudied orphan receptor required for osteoblast differentiation, identification of ligands that induce GPRC5C signaling may support therapeutic strategies to mitigate bone-related disorders.

Graphics Abstract

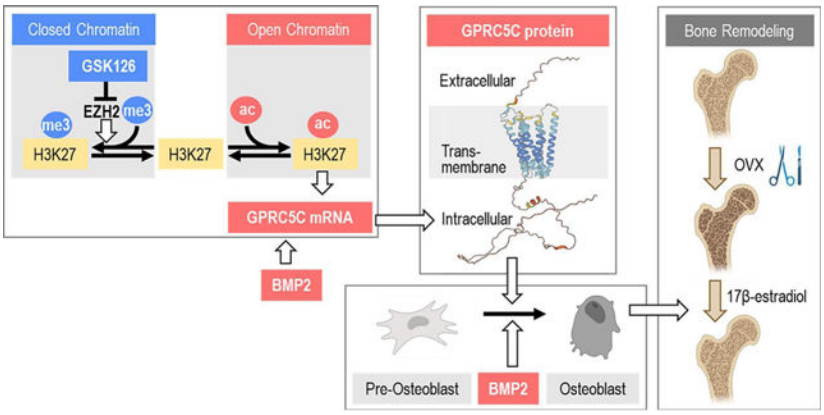

Keywords

G protein coupled receptor; GPRC5C; EZH2; BMP2; cell signaling; epigenetics; osteoblast; bone; histone methylation

INTRODUCTION

Bone formation is mediated by the intricate interplay between secreted endocrine and paracrine ligands (e.g., BMPs, PTH, WNTs, FGFs), their cognate receptors, and nuclear effector proteins such as transcription factors (e.g., RUNX2, SP7/Osterix, DLX5), coactivating proteins (e.g., SMADs, β-catenin) and epigenetic regulators (e.g., HDACs, EZH2) [1]. These osteoblast-related molecular mechanisms can be clinically targeted using a range of bioreagents including recombinant proteins, neutralizing antibodies and small molecule inhibitors. Therefore, characterization of novel molecular targets is relevant to clinical conditions characterized by low bone mineral density, including osteoporosis and osteopenia, which is a precursor to osteoporosis [2]. Several boneanabolic drugs (e.g., Teriparatide, Abaloparatide, Romosozumab) are currently utilized to treat osteoporosis, but these therapies have clinical limitations [3]. For example, use of the PTH-related protein Teriparatide is limited to 18–24 months of treatment to reduce adverse effects, while the SOST-antibody related Romosozumab is restricted due to cardiovascular and cerebrovascular complications [3, 4]. Hence, novel pharmacotherapies that encourage local bone production (e.g., nonunion fractures) or counteract bone degeneration (e.g., osteoporosis) would address unmet clinical needs.

Osteoblast differentiation is regulated by the osteogenic master regulator RUNX2 [5–8], as well as by epigenetic enzymes and architectural proteins that control chromatin structure

by depositing, removing or interpreting post-translational modifications (PTMs) of histone proteins [1, 9]. Mouse gene knockout studies, loss of function studies in cell culture and/or mechanistic omics studies with mesenchymal stem cells or osteoblasts have shown that multiple epigenetic regulators have key functions during osteoblast differentiation. Vitamin C dependent DNA hydroxylases (e.g., TET1, TET2) alter cytosine methylation and hydroxymethylation in DNA [10–13] and mediate activation of bone specific genes. Histone acetyl transferases (e.g., p300/EP300) [14] and acetylreading bromodomain proteins support osteoblast differentiation (e.g., BRD2, BRD4) [7, 15–19]. Histone deacetylases (e.g., HDAC3, HDAC5, HDAC6) modulate osteoblast and osteocyte differentiation [20–25]. For example, HDAC3 in mice is required for fidelity of lineage-selection in osteochondroprogenitors [26] and maintenance of bone mass [27, 28], while HDAC5 controls sclerostin expression in osteocytes [25]. Beyond histone acetylation, a number of histone methyl transferases (e.g., EZH2, SUV420H2, SMYD2, PRMT5, G9A/EHMT2) [6, 29–35], histone demethylases (e.g., LSD1, KDM4B, KDM6A, KDM6B) [12, 29, 35, 36] and chromodomain proteins (e.g., CHD1, CBX2) [37–39] regulate osteoblastogenesis.

EZH2 is a critical epigenetic regulator that controls bone formation and mineralization during skeletal development and mesenchymal cell growth and differentiation [40–46]. Ezh2 maintains the uncommitted state of mesenchymal stem cells (MSCs) while suppressing the osteogenic fate of stem cells required for osteogenesis [46, 47].The enzymatic activity of EZH2 suppresses osteogenesis by catalyzing histone H3 lysine 27 mono-, di-, and trimethylation (H3K27me1, H3K27me2, and H3K27me3) [32, 43–46, 48–53]. The accumulation of H3K27me3 marks mediates chromatin compaction to repress gene expression [54]. Both pharmacological and miRNA based strategies to inhibit EZH2 have been considered to promote bone formation in different models [48, 49, 52]. Inhibition of EZH2 activity enhances osteogenic lineage commitment and osteoblast differentiation *in vitro* and promotes bone formation *in vivo* [42, 49, 55–57]. Mechanistically, EZH2 inhibition enhances expression of established bone-related genes and genes involved in osteogenic signaling pathways (e.g., WNT, PTH and BMP2 pathways) that promote phosphorylation of SMAD1/5 (BMP2 signaling) [41–43, 58]. RNA-seq and ChIP-seq data show that WNT10B and PTH1R are both epigenetically activated by EZH2 inhibition [59]. WNT signaling promotes osteogenic differentiation via epigenetic derepression of the BMP2 promoter by loss of DNA methylation [42], while EZH2 inhibition activates endogenous BMP-signaling (i.e., SMAD5 phosphorylation) [59].

Gene regulatory mechanisms in the nucleus controlling osteogenic differentiation operate concurrently with changes in regulatory receptors at the cell surface that may respond to other osteogenic paracrine signals. The BMP2 responsive transcription factor RUNX2 controls osteoblast differentiation in part by regulating the expression of G protein coupled receptors, including the non-genomic estrogen receptor GPR30/GPER1 [60]. EZH2 inhibition stimulates BMP2 signaling and RUNX2 protein levels [30]. One major target for EZH2 inhibition is the PTH1R gene [42], which encodes a G protein coupled receptor that is linked to multiple heterotrimeric G proteins, including Gs and Gq/11 [61]. Furthermore, studies on the role of EZH2 as an essential epigenetic suppressor of osteoblastogenesis demonstrated that EZH2 inhibition enhances the osteogenic effects of BMP2 [55]. Co-administration of BMP2 with the EZH2 inhibitor GSK126 (iEZH2)

synergistically stimulates osteogenic differentiation [40]. RNA-sequencing indicates that in addition to promoting expression of key osteogenic genes (e.g., BGLAP/osteocalcin and IBSP/bone sialoprotein), the combination of BMP2 and GSK126 synergistically activates expression of multiple other genes, including the PTH1R gene [42]. The question arises whether stimulation of osteogenic differentiation by EZH2 inhibitors involves stimulation of G protein coupled receptors beyond PTH1R.

Here, we investigated whether and how the expression of all annotated G protein coupled receptor related genes is controlled by both EZH2 inhibition and BMP2 exposure in osteoblasts. These findings revealed that beyond the PTH responsive receptor PTH1R and the RUNX2 responsive non-genomic estrogen receptor Gpr30/GPER, the expression of the putative retinoic responsive orphan receptor GPRC5C/RAIG3 is also modulated. Analysis of the functional contribution of GPRC5C to Vitamin C induced osteoblast differentiation, alone or in the context of EZH2 inhibition and BMP2 treatment, revealed that GPRC5C is required for basal and accelerated (i.e., BMP2 and iEZH2 stimulated) acquisition of the osteoblast phenotype.

MATERIALS & METHODS

MC3T3 Cell Culture and Differentiation

The immortalized and well-characterized murine pre-osteoblast MC3T3 E1 sc4 cell line (referred to as MC3T3-E1 osteoblasts) was purchased from American Type Culture Collection [62]. Cells were maintained in α-minimal essential medium (α-MEM) without Vitamin C (ascorbate; Gibco) containing 10% fetal bovine serum (Atlanta Biologicals), 100 units/ml penicillin, and 100 μg/ml streptomycin (Gibco). For osteogenic differentiation, cells were seeded in maintenance medium at a density of 10,000 cells/cm^2. This medium was replaced on the following day by osteogenic medium supplemented with vehicle, GSK126 (5 μM; Xcess Biociences Inc.) and/or recombinant human/mouse/rat BMP2 (10 or 50 ng/ml; R&D Systems). Osteogenic medium for MC3T3-E1 cells consisted of α-MEM containing Vitamin C (50 μg/ml; Sigma) and β-glycerol phosphate (4 mM; Sigma) and was replenished after three days. On day 6 of differentiation, fresh osteogenic medium without GSK126 or BMP2 was added and replenished every 2 to 3 days.

Gprc5c gene silencing by short hairpin RNA (shRNA) in MC3T3-E1 cells

Loss-of-function studies were performed in MC3T3-E1 cells that were stably transduced with lentivirally-encoded shRNAs that target *Gprc5c*. Lentiviral vectors were generated using HEK293 packaging cells (System Biosciences) that were co-transfected with MISSION TRC2-pLKO-puroR vectors (Sigma; empty vector control (EVCtrl), scramble shRNA (NegCtrl) or anti-Gprc5c shRNAs), packaging plasmid psPAX2 (Addgene plasmid #12260) and envelope plasmid pMD2.G (Addgene plasmid #12259) with Fugene transfection reagent (Promega). Lentiviral supernatants were collected at 48, 72 and 96 hours. MC3T3-E1 cells were transduced three times by spin infection with lentiviruses with a time gap of 24 hr. Cells expressing the lentiviral-encoded puromycin resistance gene (puroR) were selected by treatment with puromycin (1 μg/ml; Santa Cruz) after the third

infection. Efficiencies of shRNA knockdowns were evaluated by RTqPCR and western blot analyses.

RNA isolation and quantitative real-time reverse transcriptase PCR (RT-qPCR).

Cells were lysed using TRIzol Reagent (Invitrogen) and RNA was isolated using the Direct-zol RNA MiniPrep Kit (Zymo Research) with an on-column DNA digestion kit (Zymo Research). Isolated RNA was reverse transcribed into cDNA using the SuperScript III First Strand Synthesis System (Invitrogen). Gene expression was quantified using real-time PCR in which each reaction was performed with 10 ng cDNA per 10 μl, QuantiTect SYBR Green PCR Kit (Qiagen), and the CFX384 Real-Time System machine (BioRad). Transcript levels were quantified using the $2^{-\Delta\Delta Ct}$ method and normalized to the housekeeping gene Gapdh. We used the following gene secific primers: Gprc5c: F-GGCTATGAGACCATCCTGAAGG, R-CAGCTGTCCATTGTAGCCACTG; Bglap: F-GCAATAAGGTAGTGAACAGACTCC, R-CCATAGATGCGTTTGTAGGCGG; Ibsp: F-GAATGGCCTGTGCTTTCTCG, R-CCCGTACTTAAAGACCCCGTT; Sp7: F-GAGGCAACTGGCTAGGTGG, R-CTGGATTAAGGGGAGCAAAGTC; Gapdh: F-CATCACTGCCACCCAGAAGACTG, R-ATGCCAGTGACTTCCCGTTCAG.

High throughput RNA sequencing, ChIP-seq data and bioinformatic analysis

RNA sequencing results presented in this study were obtained in our institutional RNA sequencing core facility and processed by institutional bioinformatics experts. RNA samples were indexed using TruSeq Kits and subjected to paired-end sequencing (HiSeq 2000 sequencer) with quality control of the indexed libraries (i.e., Bioanalyzer DNA 1000 chip, Agilent; and Qubit fluorometry, Invitrogen). Read alignments and normalized gene counts expressed as fragments per kilobasepair per million mapped reads (FPKM) were established with the MAP-RSeq (v.1.2.1) pipeline with TopHat and HTSeq as described previously [12, 30, 63].

We also queried RNA-seq data from human musculoskeletal tissues including bone, cartilage, growth plate, muscle, and adipose tissue, as well as different cell types and biological conditions that were generated in previous studies from our group [12, 30, 63]. RNA-seq data of differentiating MC3T3-E1 cells treated with vehicle, GSK126, BMP2, or the combination of GSK126 and BMP2 [55] were analyzed to assess iEZH2 and BMP2 response of GPRC-related proteins. Singular RNA-seq determinations were obtained for samples in which RNA from three biological replicates were pooled. In our experience, technical duplicates for pooled cell lines samples typically provide nearly identical results. Our RNA-seq data are accessible in the Gene Expression Omnibus of the National Center for Biotechnology Information (GSE135984) or provided as Supplementary Data in a previous study [30]. Additional expression data for muscle samples were obtained from the Sequence Read Archive database (i.e., SRR1424734 and SRR1424735). RNA-seq data for undifferentiated mouse bone marrow-derived mesenchymal stem cells (BMSC) grown in advanced minimal essential medium (MEM) 10% fetal bovine serum and 100 μg/mL penicillin/streptomycin were characterized previously [64]

RNA-seq data from ovariectomized mice and Klf10 null mice were presented in a previous paper [14]. In brief, Gprc5c gene expression was examined in littermates of crosses between heterozygous mice with a Klf10/Tieg null mutation (~8–9 weeks) [65]. These mice exhibit a female-specific osteopenic bone phenotype [66, 67] and impaired BMP2 signaling [68]. Grpc5c gene expression was also monitored in estrogen deficient wild type mice. These mice were subjected at ~6 weeks of age to either sham surgery or ovariectomy, and then were maintained for ~4 weeks without (placebo) or with estrogen replacement that was supplied via subcutaneous pellets that permit sustained release of 17β-estradiol (1.88μg) [65]. Total RNA was isolated from either cortical or trabecular bone of each mouse model (triplicate samples) and subjected to RNA-seq analysis as described previously [65].

All analyses of RNA-seq data presented in this study were obtained using comparable procedures and processed using a standard bioinformatic pipeline as described previously [42]. Publicly available ChIP-seq data from our research group in MC3T3-E1 cells in the presence or absence of GSK126 [42] were consulted to visualize the levels of H3K27me3 at the locus for the Ezh2 responsive Gprc5c gene.

Western Blot Analysis

Whole cell protein extracts were prepared using SDS sample buffer (2% SDS, 100 mM β-mercaptoethanol, and 125 mM Tris-HCl, pH 6.8). Lysates were cleared by centrifugation. Protein concentrations were determined by the DC Protein Assay (Bio-Rad). Proteins were heated at 95 °C for 5 min and resolved by SDS-PAGE and transferred to polyvinylidene difluoride membranes. After blocking in 5% nonfat dry milk for 90 min at room temperature, primary antibodies were added overnight at 4 °C, followed by secondary antibodies for 1 h at room temperature. Proteins were visualized using an ECL Prime detection kit. The primary antibodies used in western blot experiments were GPRC5C (1:1000; ab75499; Abcam), GAPDH (1:1000; 5174S; Cell Signalling), H3K27me3 (1:1000; Millipore; Cat #ABE44), H3K27ac (1:1000; Millipore; Cat #17–683), AKT1 (1:1000; Cell Signaling; mAb #2938) and β-tubulin (Tubb) (Developmental Studies Hybridoma Bank; Iowa City, Iowa; Cat #E7, 1:10,000).

Alizarin Red Staining

Alizarin Red staining was performed to assess calcium deposition in differentiated cultures. Cells were fixed in 10% neutral buffered formalin and stained with 2% Alizarin Red (Sigma) to visualize calcium deposits. Absorption of Alizarin Red stain was quantified with ImageJ software [55].

Statistics

Data are shown as mean ± standard deviation (STD). All numerical analyses of the results were evaluated for statistical significance using standard algorithms in Prism (GraphPad Software, San Diego, CA) at probability values below 0.05 ($p<0.05$). Significance was determined by ANOVA and indicated by asterisks (* = $p<0.05$; ** = $p<0.01$; *** = $p<0.001$, and **** = $p<0.001$).

RESULTS

Identification of Gprc5c as a novel G-protein coupled receptor associated with osteoblast differentiation.

We established that BMP2 treatment and Ezh2/EZH2 inhibition (GSK126) synergistically stimulate osteogenic differentiation of MC3T3-E1 pre-osteoblasts and human bone-marrow derived mesenchymal stem cells (hBMSCs) [44]. Because inhibition of EZH2 protein involves stimulation of G-protein coupled cell surface receptor proteins (e.g., PTH1R), we investigated whether the nuclear epigenetic function of EZH2 suppresses other G-protein coupled receptors (GPRs or GPRCs) during BMP2induced osteogenic differentiation. Therefore, we examined the RNA-seq expression profiles of all proteins that by gene ontology terms are linked to G-protein coupled receptor signaling (including cell surface receptors, G proteins and other associated proteins; n=459) in differentiating (days 1 and 6) MC3T3-E1 cells (Fig. 1A). Cells were treated on day 0 and day 3 with BMP2 (10 vs 50 ng/ml) in the absence or presence of the EZH2 enzyme inhibitor GSK126 (5 μM). The two doses of BMP2 were selected because 50 ng/ml of BMP2 represents an optimal dose that maximizes expression of bone marker gene expression and ECM mineralization of MC3T3-E1 cells, while 10 ng/ml BMP2 is a suboptimal dose that permits observation of synergistic effects between BMP2 and GSK126. We have observed that 10 ng/ml BMP2 plus 5 μM GSK126 is approximately equivalent to 50 ng/ml of BMP2 [44].

Heatmap analysis for all robustly expressed proteins related to GPRC signaling (average expression: FPKM>1; n=115; Suppl. Table S1) revealed two classes of transcripts that are either more abundant in early differentiated cells (day 6; Clades I-III) or in proliferating cells (day 1; Clades IV & V). Clades II and III both represent groups of differentiation related genes. Clade II genes were deprioritized because these genes either do not exhibit major changes upon BMP2 or GSK126 treatment, or they are suppressed by BMP2 and/or GSK126 (Suppl. Fig. S1 & Suppl. Table S2). Importantly, Clade III genes (n=14) are expressed at low levels in undifferentiated osteoblasts (day 1) but are elevated during early stages of osteoblastogenesis (at day 6), upregulated with either 10 or 50 ng/ml of BMP2, or further stimulated by GSK126 treatment (5 μM) (Suppl. Fig. S2 & Suppl. Table S3). Among the 14 genes in Clade III, we find Pth1r as expected, as well as the WNT related receptors Fzd5 and Fzd8, the Runx2 responsive receptor Gpr30/Gper1, the JAK/STAT-related Jak2 receptor and the orphan receptor Gprc5c (Figs. 1B&C; Suppl. Fig. 2). Pth1r and Gprc5c represent the highest expressed and most prominently induced receptors in MC3T3 at day 6 upon treatment with both BMP2 and GSK126. While Pth1r has been well studied, there are limited studies on Gprc5c, which is a member of a family of four related Gprc5 proteins (Fig. 1D&E).

Focusing on Gprc5c expression, we examined additional RNA-seq data for hypothesis building and to illustrate expression trends consistent with the differentiation-related expression of Gprc5c. We note that Gprc5c mRNA levels were enhanced by GSK126 (5 μM) treatment during osteogenic differentiation (Fig. 2A). Low (10 ng/ml) and high (50 ng/ml) concentrations of BMP2, and GSK126 (5 μM) alone induced Gprc5c expression (Suppl. Fig. 2). Furthermore, the combination of these two pro-osteogenic stimuli potentiated the

upregulation of Gprc5c expression as measured by RNA-seq at six days after Vitamin C dependent induction of MC3T3-E1 osteoblasts differentiation. Gprc5c was upregulated in post-confluent cells in the presence of Vitamin C (Fig. 2B) and is the only Gprc5 member that was upregulated during differentiation of MC3T3-E1 osteoblasts (Fig. 2C). ChIP-seq data from MC3T3-E1 cells [42] revealed that H3K27me3 levels at the Gprc5c locus were reduced after GSK126 treatment (Fig. 2D). This result is consistent with ENCODE data (UCSC Genome Browser) near the transcriptional start site (TSS) of the human GPRC5C gene. This TSS region contains high levels of H3K27ac when the gene is actively expressed (data not shown). Because H3K27ac is antagonized by H3K27me3, the presence of this mark provides a mechanistic reason for why the mouse Gprc5c gene is activated by Ezh2 inhibition. Taken together, we propose that the Gprc5c gene is a direct target of Ezh2 protein and subjected to formation of facultative heterochromatin by H3K27me3.

Follow-up RT-qPCR and RNA-seq analyses revealed that, similar to the osteoblast transcription factor (Sp7/Osterix) and principal bone related genes Bglap and Ibsp, Gprc5c was up-regulated during osteogenic differentiation of MC3T3-E1 cells (Fig. 3 and Suppl. Fig. S3). These data together indicated that the differentiation related enhancement of Gprc5c expression is linked to mature Bglap positive MC3T3-E1 cells. While we observed that Gprc5c is induced by Vitamin C, BMP2 and Ezh2 inhibition, this protein was initially described as Retinoic Acid Inducible Gene 3 (RAIG-3) [63]. However, treatment of MC3T3-E1 cells with all-trans retinoic acid did not result in appreciable changes in Gprc5c mRNA levels (Suppl. Fig. S4). MC3T3-E1 cells are derived from mouse calvaria, and indeed Gprc5c is highly expressed in mouse calvaria isolated from 3 days old pups (e.g., compared to Gprc5b and Gprc5a) (Fig. 4A), consistent with its differentiation specific expression in MC3T3-E1 cells (Fig. 3). The Gprc5c gene is expressed at low levels in undifferentiated ATDC5 chondrogenic teratoma cells and clearly expressed in C2C12 pre-myoblastic cells (Suppl. Fig. S5). Gprc5c mRNA was barely detected in mouse bone marrow derived mesenchymal stromal cells (BMSCs) (Fig. 4B), which are progenitors that give rise to many of terminally differentiated musculoskeletal cells, including osteoblasts. In agreement with this finding, Gprc5c mRNA was readily detected in human musculoskeletal tissue specimens (bone, cartilage, growth plate, and muscle), but not in human BMSCs that are in very early stages of osteogenic differentiation (Suppl. Fig. S6). Taken together, these results demonstrate that Gprc5c expression is enhanced during early stages of Vitamin C induced osteoblast differentiation and this stimulation is augmented by BMP2 treatment and Ezh2 inhibition.

One key mechanism by which EZH2 inhibition enhances osteogenesis is by increasing endogenous BMP signaling, which controls the BMP2/SMAD/RUNX2/SP7 axis. We investigated whether this activation of endogenous BMP signaling is mediated through increased receptor expression. We examined expression of a panel of BMP/activin receptors (i.e., Bmpr1a, Bmpr1b, Bmpr2, Acvr1, Acvr1b, Acvr1c, Acvr2a, Acvr2b). Our RNA-seq data show that two of these genes (i.e., Bmpr1b, Acvr1c) are not expressed, while the other six genes are expressed but their expression does not appreciably respond to BMP2 or to EZH2 inhibition (Suppl. Table S4). Hence, activation of endogenous BMP2/phospho-Smad1/5 signaling is not mediated by changes in BMP receptor mRNA levels, but rather facilitated by other osteogenic pathways.

Gprc5c knockdown impairs differentiation of MC3T3-E1 pre-osteoblasts.

To investigate the role of Gprc5c during osteoblast differentiation, we conducted loss of function studies using shRNA-mediated mechanisms to generate MC3T3 cell lines in which Gprc5c expression is suppressed at the protein level (Fig. 5A). Both Gprc5c shRNA knockdown cells, and negative control cells, were cultured in osteogenic medium. RT-qPCR analysis indicated that essential osteogenic mRNA markers, including Bglap, Ibsp, and Alpl, were suppressed in Gprc5c shRNA knockdown cells when compared to controls (Fig. 5B). These results indicate that Gprc5c is an upstream factor required for expression of these osteoblast markers.

Because Gprc5c is activated by Ezh2 inhibition, we investigated whether there is feedback regulation between Grpc5c and Ezh2. Interestingly, loss of Gprc5c decreases total nuclear H3K27ac levels, while increasing Ezh2 dependent H3K27me3 levels (Suppl. S7). This finding suggests that the Gprc5c gene, once de-repressed by Ezh2 inhibition, modulates the dynamic equilibrium between H3K27 methylation and demethylation, in favor of the latter to support of H3K27 acetylation.

Because Gprc5c and many osteoblast-specific markers are BMP2 responsive, we also examined the effect of silencing Gprc5c in cells treated with BMP2 (Suppl. Fig. S8 & Suppl. Table S5). The results show that Sp7/Osterix mRNA and Bglap/Osteocalcin are BMP2 responsive, as predicted. However, only the mRNA levels of Bglap and not Sp7 are reduced in the presence of shGprc5c. For comparison, Ibsp/bone sialoprotein mRNA is not BMP2 responsive, but its levels are suppressed by shGprc5c. This result suggests that Gprc5c is downstream of BMP2 signaling but not rate-limiting for the effects of BMP2 on Osterix/Sp7.

To assess the contribution of Gprc5c on accelerated MC3T3 osteogenic differentiation, Gprc5c was depleted in the presence or absence of 5 μM GSK126 or 50 ng/ml BMP2, which are two potent osteogenic stimuli. These data showed that Gprc5c depletion suppressed osteogenic differentiaiton as evaluated by RT-qPCR for osteogenic genes (i.e., Ibsp and Bglap) and mineral depositon by alizarin red staining (Suppl. Fig. S9). Next, we investigated the effects of Gprc5c depletion on the differentiation potential of MC3T3 treated with GSK126 (5 μM) in combination with BMP2 (50 ng/ml). These studies revealed that Gprc5c was induced by dual GSK126 and BMP2 administration, which was robustly suppressed by shRNA-mediated Gprc5c depletion (Fig. 6A). Similarly, dual GSK126 and BMP2 administration enhanced expression of key osteoblast markers, Bglap and Ibsp, and this effect was reduced by Gprc5c depletion (Fig. 6A). In support of earlier studies, depletion of Gprc5c impeded mineral depositon in vehicle treated cells (Fig. 6B&C). Importantly, the enhancement in mineral depositon by dual GSK126 and BMP2 administration was significantly impeded upon the depletion of Gprc5c (Fig. 6B&D).

Our previous study established that synergistic induction of osteogenic differentiation is most prominent upon combined administration of GSK126 (5 μM) and a low concentration of BMP2 (10 ng/ml) [44]. The introduction of GSK126 drastically reduced the amount of BMP2 required to stimulate osteogenic differentiation (from 50 ng/ml to 10 ng/ml). We assessed whether Gprc5c depletion also impacts osteoblast differentiation by the synergistic

cocktail of 5 μM GSK126 and 10 ng/ml BMP2. Synergistic induction of Gprc5c was observed upon dual administration of GSK126 and low BMP2 concentration, which was prevented by Gprc5c targeting shRNAs on day six of osteogenic differentiation (Suppl. Fig S10A). Similarly, the expression of the osteoblast marker Bglap was potentiated by dual administration of GSK126 and low BMP2 concentration, but this modulation was prevented by Gprc5c depletion. Similar to Bglap expresion, mineral deposition, as evaluated by alizarin red staining, was increased by the combination of GSK126 and BMP2 (Suppl. Fig S10B&C). However, this increase was completely abolished by the depletion of Gprc5c. These studies establish that Gprc5c is synergistically activated by Ezh2 inhibition and BMP2 treatment. Furthermore, these studies demonstrate that Gprc5c is required for osteoblast differentiation in culture and this requirement is more prominent and persists even in the presence of strong osteogenic inducers such as GSK126 and BMP2.

Gprc5c expression is reduced in osteopenic mice.

For future consideration of Gprc5c protein as target for bone anabolic strategies, it is necessary to establish that Gprc5c expression is robustly expressed in cortical and trabecular bone of osteopenic mouse models. Therefore, we first examined RNA-seq data to understand how Gprc5 family expression changes in female littermates of wild type mice versus Tieg1/Klf10 null mice (at 12 weeks) that exhibit deregulation of BMP2 signaling and Runx2 expression [65, 68] (Fig. 7A). Female but not male Tieg1/Klf10 null mice are osteopenic and this sex-specific phenotype persists for at least 12 months with no apparent genotype-dependent changes in bone with age [65, 68]. We analyzed levels of the Gprc5 family in parallel with the levels of Pth1r mRNA, which encodes the bone anabolic PTH receptor that is normally suppressed by Ezh2, and Gpr30 mRNA, which encodes the non-genomic estrogen receptor. Loss of Klf10 expression in mice reduced Gprc5c expression in trabecular, but not in cortical bone (Fig. 7B&C). Similar trends were observed in the expression patterns for Pth1r and Gpr30. This *in vivo* observation is consistent with our cell culture studies showing that Gprc5c is a BMP2 responsive gene.

We also examined RNA-seq data from cortical or trabecular bone from mice that were estrogen-depleted by ovariectomy (OVX) (Fig. 8A). A cohort of mice subjected to OVX (at 2 months) were subequently treated with estrogen for 1 month to assess bone anabolic responses in this osteopenia model (at 3 months) [65] with RNA-seq analysis at 3 months old. Under these conditions, we observed estrogen-induced expression of Pth1r and Gpr30, and the upregulation of both mRNAs was only observed in trabecular bone and not cortical bone (Fig. 8B&C). Cortical and trabecular bone from Control and OVX mice selectively express three of the four Gprc5 gene subtypes with the following order of expression: Gprc5c>Gprc5b>Gprc5a, similar to findings obtained for mature differentiated MC3T3-E1 osteoblasts in culture (see Fig. 2C). Strikingly, stimulation of OVX mice with 17β-estradiol selectively stimulated Gprc5c but not Gprc5b or Gprc5a. This estrogen effect was also only observed in trabecular bone. These data demonstrate that Gprc5c is expressed in trabecular bone of osteopenic OVX mice and is activated as part of an estrogen-mediated bone anabolic response.

To understand the differences in gene expression signatures for Gprc5c in cortical versus trabecular bone, we examined the expression of proliferation markers, as well as early and later markers of osteogenesis (Suppl. Fig. S11). These results show that trabecular bone specimens under normal and OVX conditions in general express higher levels of proliferation markers (e.g., Mki67/Ki-67 antigen, Ccna2/cyclin A, Ccnb1/cyclin B) but lower levels of early and late bone ECM markers (e.g., Col1a1 & Col1a2, Alpl, Ibsp, Spp1 and Bglap) in either wild type or Klf10 null mice. Consistent with these differences, we find that Ezh2 mRNAs levels are higher in trabecular bone than in cortical bone, while Ezh1 appears to be expressed at similar levels in cortical and trabecular bone in both wild type or Klf10 null mice (Suppl. Fig. S12). These data suggest that trabecular bone may have a greater proportion of proliferating immature osteoblast that reside on the surface of the trabeculae, compared to cortical bone which appears to be enriched for expression signatures of resting mature osteoblasts and osteocytes. Interestingly, 17β-estradiol treatment of OVX mice selectively and significantly decreases Ezh2 mRNA levels (Suppl. Fig. S12). Notably, this 17β-estradiol dependent decrease in Ezh2 mRNA levels correlates with increased expression of bone markers (Suppl. Fig. S11), consistent with the well-established pro-osteogenic effects of Ezh2 inhibitors on osteogenic differentiation and the concomitant increased expression of Gprc5c mRNA (Fig. 8B&C).

DISCUSSION

Ezh2, the catalytic protein of polycomb repressive complex 2 (PRC2), is essential for normal skeletal development and is a suppressor of early stages of bone formation [42–44]. Inhibition of Ezh2 (e.g., by GSK126) encourages mesenchymal precursor cells to commit to the osteogenic lineage and accelerate osteoblast maturation [51, 54]. Transcriptome and epigenome studies have shown that Ezh2 inhibition stimulates signaling by BMPs, which are among one of the most potent pro-osteogenic factors known [69–72]. We have demonstrated that the combination of BMP2 and Ezh2 inhibition (GSK126) results in a significant co-stimulation of MC3T3 differentiation [44]. BMP2 is currently being used in orthopedic applications to support healing of non-union fractures and spine fusion [73]. Despite its efficacy, high-concentrations of BMP2 have limited clinical applications due to their high cost [74] and negative side effects such as heterotopic ossification, osteolysis, and airway obstruction [75, 76]. Thus, there is a compelling clinical need to develop new anabolic drugs that promote bone formation and prevent bone degeneration.

This study shows that Ezh2 inhibition activates Gprc5c expression, and that the latter contributes to osteoblast maturation in culture. G-protein coupled receptors (GPCRs) are the largest family of integral membrane proteins in eukaryotes that mediate most cellular responses to hormones, neurotransmitters, olfactory cues, and taste [77, 78]. From a molecular perspective, all GPCRs are characterized by multiple membrane-spanning α-helical peptides that are flanked by intracellular and extracellular loop regions. GPCRs in vertebrates are represented by five families based on their sequence and structural similarity [79]: rhodopsin (family A), secretin (family B), glutamate (family C), adhesion and Frizzled/Taste2. Gprc5c is an orphan receptor that belongs to the Gprc5 family, which is comprised of Gprc5a, Gprc5b, Gprc5c, and Gprc5d [80–83]. Although these four receptors do not have definitely established known ligands, they have distinct tissue localization profiles. Gprc5c

has been reported mostly in the brain, liver, and kidney [63, 82, 84]. Our RNA-seq data show that Gprc5a, Gprc5b and Gprc5c, but not Gprc5d are broadly expressed at low levels in many mesenchymal cell types and tissues, but expression of Gprc5c is low in uncommitted cells and higher in differentiated osteoblasts and bone tissues.

Gprc5c has been studied primarily in dormant hematopoietic stem cells (dHSCs), the vascular system [77, 85], kidney [83], pancreatic beta-cells [86], neuroblastoma [87], intestinal cells [88], epithelial cells [89], venous thromboembolism [90], breast cancer [91], and brain [92]. Prior to this work, there were no studies on Gprc5c function in musculoskeletal tissues, including bone. The results of the current study clearly demonstrate that Gprc5c is expressed in multiple skeletal tissues including bone, cartilage, and growth plate. Our data confirms that Gprc5c mRNA is responsive to low and high doses of BMP2 and GSK126 (Ezh2 inhibitor) and the combination of both in MC3T3-E1 cells similar to that of other essential osteogenic markers. Notwithstanding our findings that Gprc5c gene expression is important for osteoblast maturation, Gprc5c knockout studies show that null mutation does not result in a dramatic bone-less phenotype but rather mice are viable, grossly normal, and fertile [84]. While an in depth analysis of the bone phenotypes was not performed by Sano and colleagues [84], our expression analysis of the four Gprc5 subfamily genes suggests that Gprc5a or Gprc5b may perhaps provide some compensation for the genetic loss of Gprc5c gene in osteoblasts, which would preclude detection of an overt bone phenotype.

Beyond the absence of an overt skeletal phenotype in Gprc5c null mice, the physiological relevance of our findings on Gprc5c is restricted by our focus on immortalized MC3T3-E1 sc4 cells as the main culture model. It will be informative to extend our present findings on the regulatory function of Gprc5c and the synergy between Ezh2 inhibition and BMP2 using wild type or genetically modified primary calvarial osteoblasts and bone marrow derived stem cells. Another limitation of our study is that we do not have a molecular comparison of bone from male and female KLF10 null mice that could potentially be interesting. However, the males do not have a phenotype and hence no molecular changes are expected when comparing Klf10 knockout and wild type mice.

Gprc5c is also known as Retinoic Acid Inducible Gene-3 (RAIG-3) [63]. This gene is responsive to all-trans retinoic acid in human astrocytoma (1321N1) and SY5Y neuroblastoma (SY5Y) cell lines, but not in human embryonic kidney fibroblasts (HEK293) or human small cell lung carcinoma (NC1-N417) cell lines [63]. We show that Gprc5c expression is also not induced by retinoic acid in MC3T3-E1 osteoblasts and is only robustly expressed in differentiated osteoblasts and following stimulation by Vitamin C, BMP2, GSK126 or 17β-estradiol. Together, these findings indicate that both basal and retinoic acid inducibility of Grpc5c are cell type and differentiation-stage dependent.

Gprc5c protein is expressed at the cell surface based on immunofluorescence microscopy analysis of non-bone cells in which the protein was over-expressed [63]. Our studies establish that this protein contributes to osteogenic differentiation of progenitor cells. Because Gprc5c is a poorly studied orphan G-protein coupled receptor, it is not entirely clear how this receptor is activated and what downstream proteins are stimulated by the

activated receptor. It is conceivable that Gprc5c protein could be modulated by small molecule inhibitors, agonists and/or monoclonal antibodies. Understanding what activates Gprc5c activity as a protein encoded by a differentiation specific and BMP2 responsive gene in osteoblasts is of considerable interest and may implicate this protein as a viable candidate for drug targeting strategies that promote osteogenesis. Recent studies on the role of Gprc5c in hematopoietic stem cells have revealed that Gprc5c may interact with hyaluronic acid [93]. Hyaluronic acid has been used in hydrogels to support osteogenic differentiation of MSCs [14]. Our studies indicate that Grpc5c mRNA is induced by BMP2, upregulated during osteoblastogenesis, and required for ECM mineralization. Collectively, these findings suggest that stimulation of Gprc5c protein by hyaluronic acid may potentially account for the osteogenic activity of hyaluronic acid in bone tissue engineering approaches. Furthermore, Gprc5c also appears to respond to saccharides and sugar alcohols [94], which would suggest that the receptor interacts with a broad range of carbohydrate ligands. It is plausible that hyaluronic acid or related (poly)saccharides could potentially be leveraged to stimulate Gprc5c protein and enhance osteoblast differentiation.

In summary, we have examined the function of Gprc5c in MC3T pre-osteoblast cells for the first time. We find that Gprc5c participates in osteoblast differentiation and its mRNA is responsive to anabolic compounds that promote bone formation. Our findings underscore the importance of the under-explored functions of orphaned GPRCs in skeletal tissues. Future research should focus on elucidating the activities of these receptors in order to uncover novel mechanisms that control osteoblastogenesis.

Supplementary Material

Refer to Web version on PubMed Central for supplementary material.

ACKNOWLEDGMENTS

We thank all members from our research group, including Eric Lewallen, Christopher Paradise, Sophia Jerez and Eva Kubrova (Mayo Clinic), as well as Hans van Leeuwen and Jeroen van de Peppel (Erasmus University) for stimulating discussions and/or providing reagents.

FUNDING

These studies were supported by NIH/NIAMS grant AR049069 (to AJvW), a career development award from the Mayo Clinic (AD), as well as a fellowship award from the Mayo Clinic Center of Regenerative Medicine (to RT) and the Patrick J. Kelly Fellowship award (to RT).

Abbreviations:

GPRC5C	G protein coupled receptor 5c
EZH2	Enhancer of zeste homolog 2
BMP2	Bone morphogenetic protein 2
RUNX2	Runt homology transcription factor 2
PTH1R	Parathyroid hormone 1 receptor

GPR30	G protein couple receptor 30
GPER1	G Protein-Coupled Estrogen Receptor 1
KLF10	Kruppel-like factor 10
SOST	Sclerostin
TET1	Ten-eleven translocation protein 1
TET2	Ten-eleven translocation protein 2
TET3	Ten-eleven translocation protein 3
OVX	Ovariectomy

REFERENCES:

1. van Wijnen AJ and Westendorf JJ, Epigenetics as a New Frontier in Orthopedic Regenerative Medicine and Oncology. J Orthop Res, 2019. 37(7): p. 1465–1474. [PubMed: 30977555]
2. Farr JN and Khosla S, Skeletal changes through the lifespan--from growth to senescence. Nat Rev Endocrinol, 2015. 11(9): p. 513–21. [PubMed: 26032105]
3. Cheng C, Wentworth K, and Shoback DM, New Frontiers in Osteoporosis Therapy. Annu Rev Med, 2020. 71: p. 277–288. [PubMed: 31509477]
4. Black DM and Rosen CJ, Clinical Practice. Postmenopausal Osteoporosis. N Engl J Med, 2016. 374(3): p. 254–62. [PubMed: 26789873]
5. Meyer MB, Benkusky NA, and Pike JW, The RUNX2 cistrome in osteoblasts: characterization, down-regulation following differentiation, and relationship to gene expression. J Biol Chem, 2014. 289(23): p. 16016–31. [PubMed: 24764292]
6. Rojas A, et al. , Mll-COMPASS complexes mediate H3K4me3 enrichment and transcription of the osteoblast master gene Runx2/p57 in osteoblasts. J Cell Physiol, 2019. 234(5): p. 6244–6253. [PubMed: 30256410]
7. Wu H, et al. , Chromatin dynamics regulate mesenchymal stem cell lineage specification and differentiation to osteogenesis. Biochim Biophys Acta Gene Regul Mech, 2017. 1860(4): p. 438–449. [PubMed: 28077316]
8. Wu H, et al. , Genomic occupancy of Runx2 with global expression profiling identifies a novel dimension to control of osteoblastogenesis. Genome Biol, 2014. 15(3): p. R52. [PubMed: 24655370]
9. Gordon JAR, et al. , Chromatin modifiers and histone modifications in bone formation, regeneration, and therapeutic intervention for bone-related disease. Bone, 2015. 81: p. 739–745. [PubMed: 25836763]
10. Cakouros D, et al. , Specific functions of TET1 and TET2 in regulating mesenchymal cell lineage determination. Epigenetics Chromatin, 2019. 12(1): p. 3. [PubMed: 30606231]
11. Sepulveda H, Villagra A, and Montecino M, Tet-Mediated DNA Demethylation Is Required for SWI/SNF-Dependent Chromatin Remodeling and Histone-Modifying Activities That Trigger Expression of the Sp7 Osteoblast Master Gene during Mesenchymal Lineage Commitment. Mol Cell Biol, 2017. 37(20).
12. Thaler R, et al. , Vitamin C epigenetically controls osteogenesis and bone mineralization. Nat Commun, 2022. 13(1): p. 5883. [PubMed: 36202795]
13. Thaler R, et al. , Anabolic and Antiresorptive Modulation of Bone Homeostasis by the Epigenetic Modulator Sulforaphane, a Naturally Occurring Isothiocyanate. J Biol Chem, 2016. 291(13): p. 6754–71. [PubMed: 26757819]
14. Gibbs DM, et al. , A review of hydrogel use in fracture healing and bone regeneration. J Tissue Eng Regen Med, 2016. 10(3): p. 187–98. [PubMed: 25491789]

15. Baud'huin M, et al. , Inhibition of BET proteins and epigenetic signaling as a potential treatment for osteoporosis. Bone, 2017. 94: p. 10–21. [PubMed: 27669656]
16. Galea GL, et al. , Mechanical strain-mediated reduction in RANKL expression is associated with RUNX2 and BRD2. Gene, 2020. 763S: p. 100027. [PubMed: 34493364]
17. Paradise CR, et al. , The epigenetic reader Brd4 is required for osteoblast differentiation. J Cell Physiol, 2020. 235(6): p. 5293–5304. [PubMed: 31868237]
18. Paradise CR, et al. , Brd4 is required for chondrocyte differentiation and endochondral ossification. Bone, 2022. 154: p. 116234. [PubMed: 34700039]
19. Shen J, et al. , Histone acetylation in vivo at the osteocalcin locus is functionally linked to vitamin D-dependent, bone tissue-specific transcription. J Biol Chem, 2002. 277(23): p. 20284–92. [PubMed: 11893738]
20. Bradley EW, et al. , Histone Deacetylases in Bone Development and Skeletal Disorders. Physiol Rev, 2015. 95(4): p. 1359–81. [PubMed: 26378079]
21. Dudakovic A, et al. , Histone deacetylase inhibition promotes osteoblast maturation by altering the histone H4 epigenome and reduces Akt phosphorylation. J Biol Chem, 2013. 288(40): p. 28783–91. [PubMed: 23940046]
22. Jafarov T, Alexander JW, and St-Arnaud R, alphaNAC interacts with histone deacetylase corepressors to control Myogenin and Osteocalcin gene expression. Biochim Biophys Acta, 2012. 1819(11–12): p. 1208–16. [PubMed: 23092676]
23. Shen J, et al. , Transcriptional induction of the osteocalcin gene during osteoblast differentiation involves acetylation of histones h3 and h4. Mol Endocrinol, 2003. 17(4): p. 743–56. [PubMed: 12554783]
24. Vrtacnik P, et al. , Epigenetic enzymes influenced by oxidative stress and hypoxia mimetic in osteoblasts are differentially expressed in patients with osteoporosis and osteoarthritis. Sci Rep, 2018. 8(1): p. 16215. [PubMed: 30385847]
25. Wein MN, et al. , HDAC5 controls MEF2C-driven sclerostin expression in osteocytes. J Bone Miner Res, 2015. 30(3): p. 400–11. [PubMed: 25271055]
26. McGee-Lawrence ME, et al. , Hdac3 Deficiency Increases Marrow Adiposity and Induces Lipid Storage and Glucocorticoid Metabolism in Osteochondroprogenitor Cells. J Bone Miner Res, 2016. 31(1): p. 116–28. [PubMed: 26211746]
27. Hesse E, et al. , Zfp521 controls bone mass by HDAC3-dependent attenuation of Runx2 activity. J Cell Biol, 2010. 191(7): p. 1271–83. [PubMed: 21173110]
28. McGee-Lawrence ME, et al. , Histone deacetylase 3 is required for maintenance of bone mass during aging. Bone, 2013. 52(1): p. 296–307. [PubMed: 23085085]
29. Clissold SP and Heel RC, Topical minoxidil. A preliminary review of its pharmacodynamic properties and therapeutic efficacy in alopecia areata and alopecia androgenetica. Drugs, 1987. 33(2): p. 107–22. [PubMed: 3552591]
30. Dashti P, et al. , The lysine methyltransferases SET and MYND domain containing 2 (Smyd2) and Enhancer of Zeste 2 (Ezh2) co-regulate osteoblast proliferation and mineralization. Gene, 2023. 851: p. 146928. [PubMed: 36191822]
31. Dudakovic A, et al. , Profiling of human epigenetic regulators using a semi-automated real-time qPCR platform validated by next generation sequencing. Gene, 2017. 609: p. 28–37. [PubMed: 28132772]
32. Dudakovic A. and van Wijnen AJ, Epigenetic Control of Osteoblast Differentiation by Enhancer of Zeste Homolog 2 (EZH2). Current Molecular Biology Reports, 2017. 3: p. 94–106.
33. Ideno H, et al. , G9a is involved in the regulation of cranial bone formation through activation of Runx2 function during development. Bone, 2020. 137: p. 115332. [PubMed: 32344102]
34. Khani F, et al. , Histone H4 Methyltransferase Suv420h2 Maintains Fidelity of Osteoblast Differentiation. J Cell Biochem, 2017. 118(5): p. 1262–1272. [PubMed: 27862226]
35. Pribadi C, et al. , Pharmacological targeting of KDM6A and KDM6B, as a novel therapeutic strategy for treating craniosynostosis in Saethre-Chotzen syndrome. Stem Cell Res Ther, 2020. 11(1): p. 529. [PubMed: 33298158]
36. Rummukainen P, et al. , Lysine-Specific Demethylase 1 (LSD1) epigenetically controls osteoblast differentiation. PLoS One, 2022. 17(3): p. e0265027. [PubMed: 35255108]

37. Baumgart SJ, et al. , CHD1 regulates cell fate determination by activation of differentiation-induced genes. Nucleic Acids Res, 2017. 45(13): p. 7722–7735. [PubMed: 28475736]
38. Katoh-Fukui Y, et al. , Mouse polycomb group gene Cbx2 promotes osteoblastic but suppresses adipogenic differentiation in postnatal long bones. Bone, 2019. 120: p. 219–231. [PubMed: 30389610]
39. van Wijnen AJ, et al. , Biological functions of chromobox (CBX) proteins in stem cell self-renewal, lineage-commitment, cancer and development. Bone, 2021. 143: p. 115659. [PubMed: 32979540]
40. Camilleri ET, et al. , Loss of histone methyltransferase Ezh2 stimulates an osteogenic transcriptional program in chondrocytes but does not affect cartilage development. J Biol Chem, 2018. 293(49): p. 19001–19011. [PubMed: 30327434]
41. Dudakovic A, et al. , Enhancer of zeste homolog 2 (Ezh2) controls bone formation and cell cycle progression during osteogenesis in mice. J Biol Chem, 2018. 293(33): p. 12894–12907. [PubMed: 29899112]
42. Dudakovic A, et al. , Enhancer of Zeste Homolog 2 Inhibition Stimulates Bone Formation and Mitigates Bone Loss Caused by Ovariectomy in Skeletally Mature Mice. J Biol Chem, 2016. 291(47): p. 24594–24606. [PubMed: 27758858]
43. Dudakovic A, et al. , Epigenetic Control of Skeletal Development by the Histone Methyltransferase Ezh2. J Biol Chem, 2015. 290(46): p. 27604–17. [PubMed: 26424790]
44. Dudakovic A, et al. , Inhibition of the epigenetic suppressor EZH2 primes osteogenic differentiation mediated by BMP2. J Biol Chem, 2020. 295(23): p. 7877–7893. [PubMed: 32332097]
45. Kobayashi Y, et al. , Ezh2 knockout in mesenchymal cells causes enamel hyper-mineralization. Biochem Biophys Res Commun, 2021. 567: p. 72–78. [PubMed: 34144503]
46. Sen B, et al. , beta-Catenin Preserves the Stem State of Murine Bone Marrow Stromal Cells Through Activation of EZH2. J Bone Miner Res, 2020.
47. Samsonraj RM, et al. , Osteogenic Stimulation of Human Adipose-Derived Mesenchymal Stem Cells Using a Fungal Metabolite That Suppresses the Polycomb Group Protein EZH2. Stem Cells Transl Med, 2018. 7(2): p. 197–209. [PubMed: 29280310]
48. Dudakovic A, et al. , MicroRNA-101a enhances trabecular bone accrual in male mice. Sci Rep, 2022. 12(1): p. 13361. [PubMed: 35922466]
49. Galvan ML, et al. , Multiple pharmacological inhibitors targeting the epigenetic suppressor enhancer of zeste homolog 2 (Ezh2) accelerate osteoblast differentiation. Bone, 2021. 150: p. 115993. [PubMed: 33940225]
50. Hemming S, et al. , EZH2 deletion in early mesenchyme compromises postnatal bone microarchitecture and structural integrity and accelerates remodeling. FASEB J, 2017. 31(3): p. 1011–1027. [PubMed: 27934660]
51. Hemming S, et al. , EZH2 and KDM6A act as an epigenetic switch to regulate mesenchymal stem cell lineage specification. Stem Cells, 2014. 32(3): p. 802–15. [PubMed: 24123378]
52. Lui H, et al. , Combination of BMP2 and EZH2 Inhibition to Stimulate Osteogenesis in a 3D Bone Reconstruction Model. Tissue Eng Part A, 2021. 27(15–16): p. 1084–1098. [PubMed: 33234056]
53. Margueron R. and Reinberg D, The Polycomb complex PRC2 and its mark in life. Nature, 2011. 469(7330): p. 343–9. [PubMed: 21248841]
54. Bouyer D, et al. , Polycomb repressive complex 2 controls the embryo-to-seedling phase transition. PLoS Genet, 2011. 7(3): p. e1002014. [PubMed: 21423668]
55. Dudakovic A, et al. , Inhibition of the epigenetic suppressor EZH2 primes osteogenic differentiation mediated by BMP2. J Biol Chem, 2020.
56. Fang C, et al. , Cutting Edge: EZH2 Promotes Osteoclastogenesis by Epigenetic Silencing of the Negative Regulator IRF8. J Immunol, 2016. 196(11): p. 4452–4456. [PubMed: 27183582]
57. Wei Y, et al. , CDK1-dependent phosphorylation of EZH2 suppresses methylation of H3K27 and promotes osteogenic differentiation of human mesenchymal stem cells. Nat Cell Biol, 2011. 13(1): p. 87–94. [PubMed: 21131960]
58. Woodhouse S, et al. , Ezh2 maintains a key phase of muscle satellite cell expansion but does not regulate terminal differentiation. J Cell Sci, 2013. 126(Pt 2): p. 565–79. [PubMed: 23203812]

59. Cho YD, et al. , Epigenetic modifications and canonical wingless/int-1 class (WNT) signaling enable trans-differentiation of nonosteogenic cells into osteoblasts. J Biol Chem, 2014. 289(29): p. 20120–8. [PubMed: 24867947]
60. Teplyuk NM, et al. , Runx2 regulates G protein-coupled signaling pathways to control growth of osteoblast progenitors. J Biol Chem, 2008. 283(41): p. 27585–27597. [PubMed: 18625716]
61. Bastepe M, Turan S, and He Q, Heterotrimeric G proteins in the control of parathyroid hormone actions. J Mol Endocrinol, 2017. 58(4): p. R203–R224. [PubMed: 28363951]
62. Wang D, et al. , Isolation and characterization of MC3T3-E1 preosteoblast subclones with distinct in vitro and in vivo differentiation/mineralization potential. J Bone Miner Res, 1999. 14(6): p. 893–903. [PubMed: 10352097]
63. Robbins MJ, et al. , Molecular cloning and characterization of two novel retinoic acid-inducible orphan G-protein-coupled receptors (GPRC5B and GPRC5C). Genomics, 2000. 67(1): p. 8–18. [PubMed: 10945465]
64. Samsonraj RM, et al. , Validation of Osteogenic Properties of Cytochalasin D by High-Resolution RNA-Sequencing in Mesenchymal Stem Cells Derived from Bone Marrow and Adipose Tissues. Stem Cells Dev, 2018. 27(16): p. 1136–1145. [PubMed: 29882479]
65. Subramaniam M, et al. , TIEG and estrogen modulate SOST expression in the murine skeleton. J Cell Physiol, 2018. 233(4): p. 3540–3551. [PubMed: 29044507]
66. Bensamoun SF, et al. , TGFbeta inducible early gene-1 knockout mice display defects in bone strength and microarchitecture. Bone, 2006. 39(6): p. 1244–51. [PubMed: 16876494]
67. Hawse JR, et al. , TIEG-null mice display an osteopenic gender-specific phenotype. Bone, 2008. 42(6): p. 1025–31. [PubMed: 18396127]
68. Hawse JR, et al. , TIEG1/KLF10 modulates Runx2 expression and activity in osteoblasts. PLoS One, 2011. 6(4): p. e19429. [PubMed: 21559363]
69. Sampath TK, et al. , Bovine osteogenic protein is composed of dimers of OP-1 and BMP-2A, two members of the transforming growth factor-beta superfamily. J Biol Chem, 1990. 265(22): p. 13198–205. [PubMed: 2376592]
70. Wang EA, et al. , Purification and characterization of other distinct bone-inducing factors. Proc Natl Acad Sci U S A, 1988. 85(24): p. 9484–8. [PubMed: 3200834]
71. Wozney JM, et al. , Novel regulators of bone formation: molecular clones and activities. Science, 1988. 242(4885): p. 1528–34. [PubMed: 3201241]
72. Yamaguchi A, et al. , Recombinant human bone morphogenetic protein-2 stimulates osteoblastic maturation and inhibits myogenic differentiation in vitro. J Cell Biol, 1991. 113(3): p. 681–7. [PubMed: 1849907]
73. Ong KL, et al. , Off-label use of bone morphogenetic proteins in the United States using administrative data. Spine (Phila Pa 1976), 2010. 35(19): p. 1794–800. [PubMed: 20700081]
74. Garrison KR, et al. , Clinical effectiveness and cost-effectiveness of bone morphogenetic proteins in the non-healing of fractures and spinal fusion: a systematic review. Health Technol Assess, 2007. 11(30): p. 1–150, iii-iv.
75. James AW, et al. , A Review of the Clinical Side Effects of Bone Morphogenetic Protein-2. Tissue Eng Part B Rev, 2016. 22(4): p. 284–97. [PubMed: 26857241]
76. Russow G, et al. , Anabolic Therapies in Osteoporosis and Bone Regeneration. Int J Mol Sci, 2018. 20(1).
77. Kaur H, et al. , Single-cell profiling reveals heterogeneity and functional patterning of GPCR expression in the vascular system. Nat Commun, 2017. 8: p. 15700. [PubMed: 28621310]
78. Rosenbaum DM, Rasmussen SG, and Kobilka BK, The structure and function of G-proteincoupled receptors. Nature, 2009. 459(7245): p. 356–63. [PubMed: 19458711]
79. Fredriksson R, et al. , The G-protein-coupled receptors in the human genome form five main families. Phylogenetic analysis, paralogon groups, and fingerprints. Mol Pharmacol, 2003. 63(6): p. 1256–72. [PubMed: 12761335]
80. Brauner-Osborne H, et al. , Cloning and characterization of a human orphan family C G-protein coupled receptor GPRC5D. Biochim Biophys Acta, 2001. 1518(3): p. 237–48. [PubMed: 11311935]

81. Brauner-Osborne H. and Krogsgaard-Larsen P, Sequence and expression pattern of a novel human orphan G-protein-coupled receptor, GPRC5B, a family C receptor with a short amino-terminal domain. Genomics, 2000. 65(2): p. 121–8. [PubMed: 10783259]
82. Cheng Y. and Lotan R, Molecular cloning and characterization of a novel retinoic acid-inducible gene that encodes a putative G protein-coupled receptor. J Biol Chem, 1998. 273(52): p. 35008–15. [PubMed: 9857033]
83. Rajkumar P, et al. , Identifying the localization and exploring a functional role for Gprc5c in the kidney. FASEB J, 2018. 32(4): p. 2046–2059. [PubMed: 29196502]
84. Sano T, et al. , Comparative characterization of GPRC5B and GPRC5CLacZ knockin mice; behavioral abnormalities in GPRC5B-deficient mice. Biochem Biophys Res Commun, 2011. 412(3): p. 460–5. [PubMed: 21840300]
85. Cabezas-Wallscheid N, et al. , Vitamin A-Retinoic Acid Signaling Regulates Hematopoietic Stem Cell Dormancy. Cell, 2017. 169(5): p. 807–823 e19. [PubMed: 28479188]
86. Amisten S, et al. , Anti-diabetic action of all-trans retinoic acid and the orphan G protein coupled receptor GPRC5C in pancreatic beta-cells. Endocr J, 2017. 64(3): p. 325–338. [PubMed: 28228611]
87. Ross RA, et al. , A distinct gene expression signature characterizes human neuroblastoma cancer stem cells. Stem Cell Res, 2015. 15(2): p. 419–26. [PubMed: 26342562]
88. Grunddal KV, et al. , Adhesion receptor ADGRG2/GPR64 is in the GI-tract selectively expressed in mature intestinal tuft cells. Mol Metab, 2021. 51: p. 101231. [PubMed: 33831593]
89. Matsui T, et al. , ALIX and ceramide differentially control polarized small extracellular vesicle release from epithelial cells. EMBO Rep, 2021. 22(5): p. e51475. [PubMed: 33724661]
90. Cunha MLR, et al. , Whole exome sequencing in thrombophilic pedigrees to identify genetic risk factors for venous thromboembolism. PLoS One, 2017. 12(11): p. e0187699. [PubMed: 29117201]
91. Yamaga R, et al. , Systemic identification of estrogen-regulated genes in breast cancer cells through cap analysis of gene expression mapping. Biochem Biophys Res Commun, 2014. 447(3): p. 531–6. [PubMed: 24746470]
92. Robbins MJ, et al. , Localisation of the GPRC5B receptor in the rat brain and spinal cord. Brain Res Mol Brain Res, 2002. 106(1–2): p. 136–44. [PubMed: 12393273]
93. Zhang YW, et al. , Hyaluronic acid-GPRC5C signalling promotes dormancy in haematopoietic stem cells. Nat Cell Biol, 2022. 24(7): p. 1038–1048. [PubMed: 35725769]
94. Kawabata Y, et al. , The G protein-coupled receptor GPRC5C is a saccharide sensor with a novel ‘off’ response. FEBS Lett, 2023.
95. Varadi M, et al. , AlphaFold Protein Structure Database: massively expanding the structural coverage of protein-sequence space with high-accuracy models. Nucleic Acids Res, 2022. 50(D1): p. D439–D444. [PubMed: 34791371]
96. Paradise CR, et al. , Molecular characterization of physis tissue by RNA sequencing. Gene, 2018. 668: p. 87–96. [PubMed: 29775757]
97. van de Peppel J, et al. , Identification of Three Early Phases of Cell-Fate Determination during Osteogenic and Adipogenic Differentiation by Transcription Factor Dynamics. Stem Cell Reports, 2017. 8(4): p. 947–960. [PubMed: 28344004]

Highlights

- The methyltransferase EZH2 epigenetically suppresses osteoblast differentiation.
- Inhibition of EZH2 and activation of BMP2 co-stimulate osteogenesis.
- This co-stimulation activates expression of the G-protein coupled receptor GPRC5C.
- GPRC5C is a key orphan receptor required for osteoblastogenesis.
- GPRC5C is induced by 17β-estradiol in trabecular bone of ovariectomized mice.

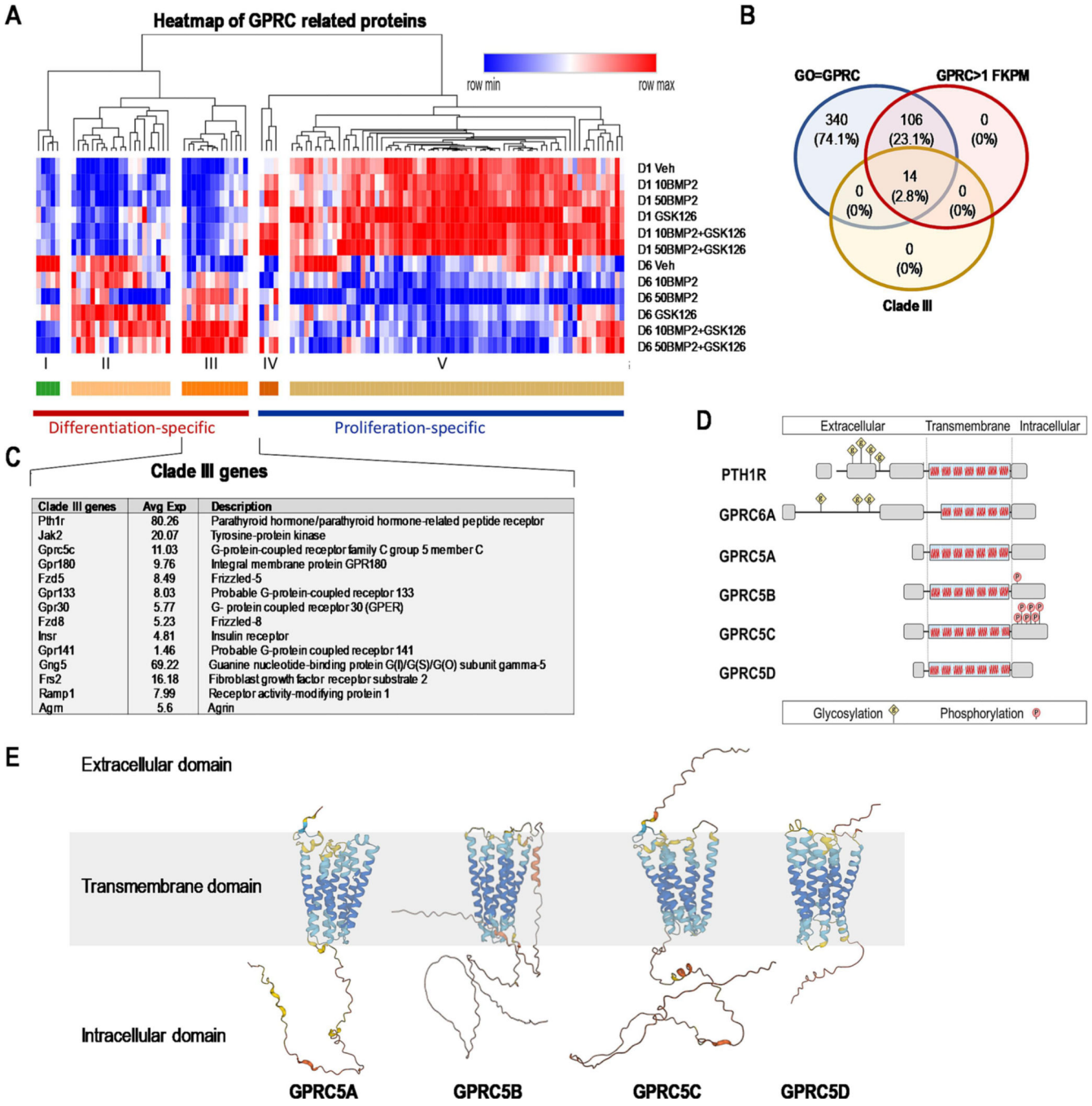

Clade III genes	Avg Exp	Description
Pth1r	80.26	Parathyroid hormone/parathyroid hormone-related peptide receptor
Jak2	20.07	Tyrosine-protein kinase
Gprc5c	11.03	G-protein-coupled receptor family C group 5 member C
Gpr180	9.76	Integral membrane protein GPR180
Fzd5	8.49	Frizzled-5
Gpr133	8.03	Probable G-protein-coupled receptor 133
Gpr30	5.77	G- protein coupled receptor 30 (GPER)
Fzd8	5.23	Frizzled-8
Insr	4.81	Insulin receptor
Gpr141	1.46	Probable G-protein coupled receptor 141
Gng5	69.22	Guanine nucleotide-binding protein G(I)/G(S)/G(O) subunit gamma-5
Frs2	16.18	Fibroblast growth factor receptor substrate 2
Ramp1	7.99	Receptor activity-modifying protein 1
Agrn	5.6	Agrin

Figure 1: RNA-seq data for Gprc5 gene expression in MC3T3-E1 cells.

(A) Heatmap of mRNAs for GPRC -related proteins by RNA-seq from differentiating MC3T3-E1 cells on day 1 (D1) and day 6 (6) treated with vehicle, GSK126, 10 or 50 ng BMP2, or combinations of GSK126 and BMP2. Gprc mRNAs were subjected to hierarchical clustering revealing five clades that differ in expression patterns. **(B)** Venn Diagram intersection between GPRC-related proteins based on GO terms (top left), GPRC proteins with expression > 1 FPKM (top right), and all GPRC proteins contained within Clade III of the heatmap (bottom). **(C)** Table with genes from Clade III (n=14 total)

that exhibit the most prominent induction or expression in MC3T3-E1 cells (FPKM). **(D)** Structure of mouse Gprc5 family proteins as indicated, with structural comparisons to the Pth1r and Gprc6a receptors. **(E)** 3D structure of intracellular, extracellular transmembrane domains within Gprc5 proteins as predicted by Alpha-fold (https://alphafold.ebi.ac.uk;) [95].

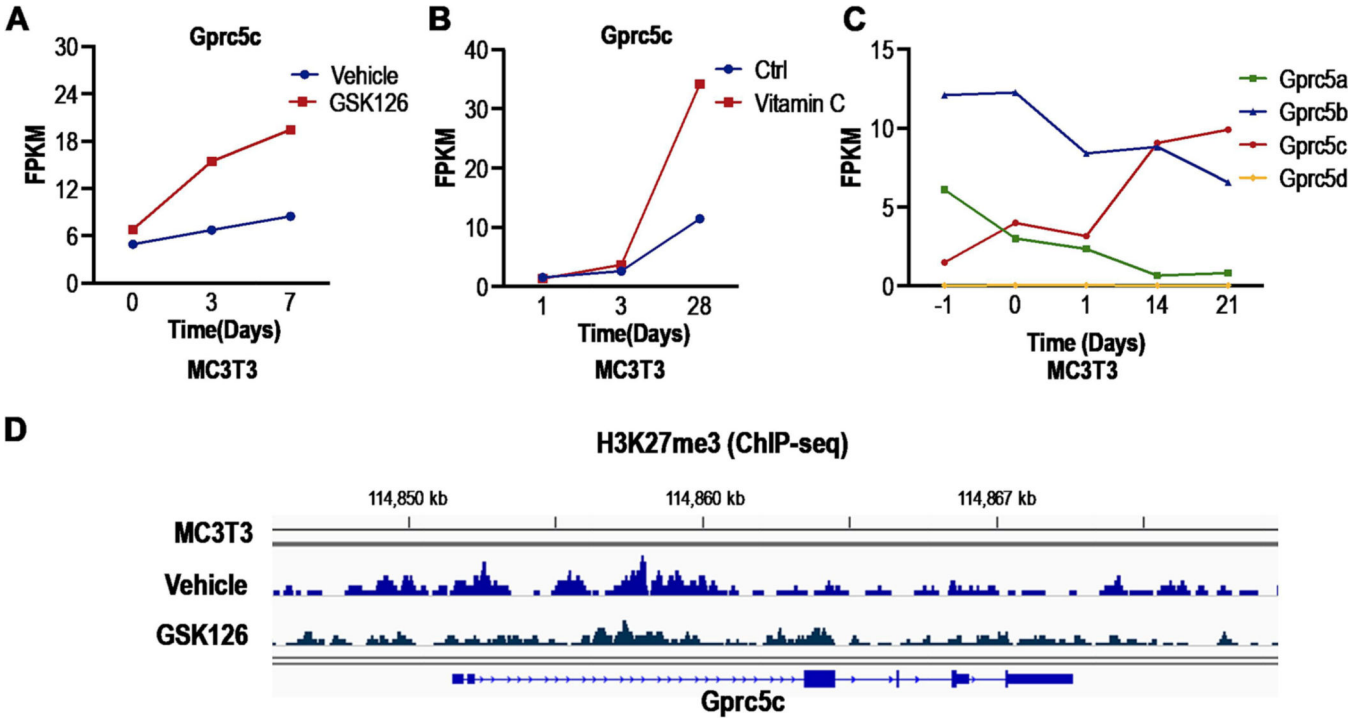

Figure 2: RNA-seq analysis of Gprc5c expression in MC3T3-E1 cells.

Gprc5c expression was examined by RNA-seq analysis from differentiating MC3T3-E1 cells **(A)** treated with vehicle and GSK126, (**B)** in the presence or absence of Vitamin C, or **(C)** a longer differentiation time course (three weeks) in comparison to other Gprc5 family members. **(D)** ChIP-seq analysis for the Ezh2-dependent modification H3K27me3 at the Gprc5c locus in MC3T3-E1 cells treated with vehicle or GSK126 for three days (tracks are on the same scale). One notable change is observed near the transcriptional start site (left side near position 114,850 kb). This approximate region is enriched for H3K27ac marks in the human GPRC5C gene in non-bone cells that express the gene. The line drawings presented in Panels A, B and C were obtained by statistically robust RNA-seq data, but each measurement represents a single RNA-seq data point on the graph. Therefore, these data are only provided for hypothesis building and to illustrate consistent expression trends for Gprc5c across multiple samples.

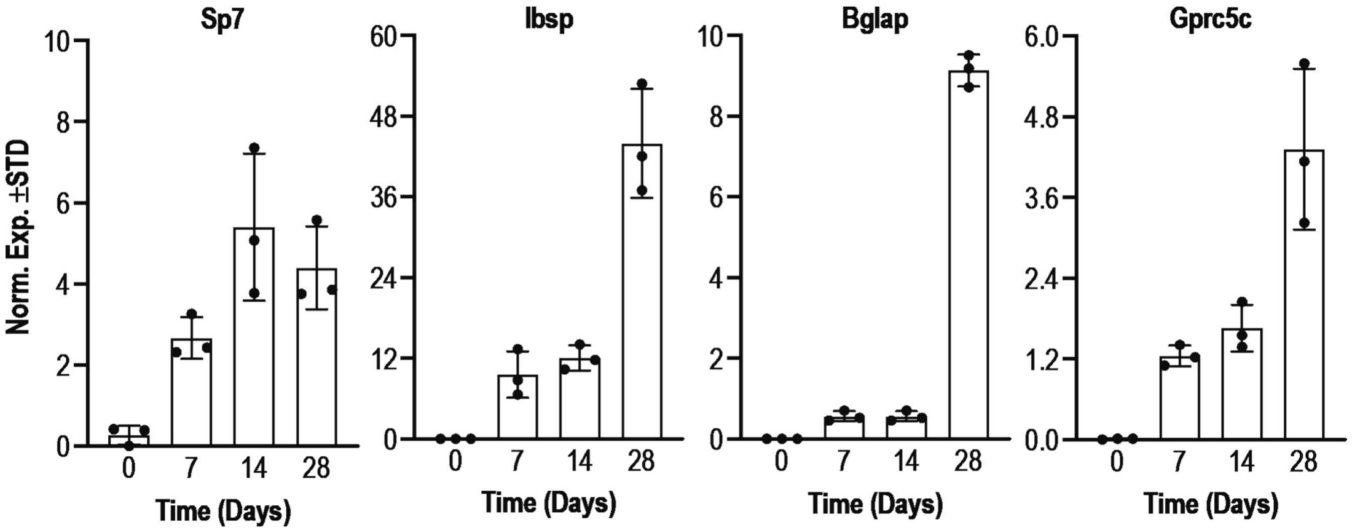

Figure 3: Gprc5c is induced during osteogenic differentiation of MC3T3-E1 cells.

RT-qPCR was used to validate expression patterns for Gprc5c during a time course of MC3T3 differentiation in relation to the osteogenic transcription factor Sp7/Osterix, and key bone markers (Bglap and Ibsp). Graphs show data from biological triplicates analyzed as technical duplicates (n = 3, mean ± STD).

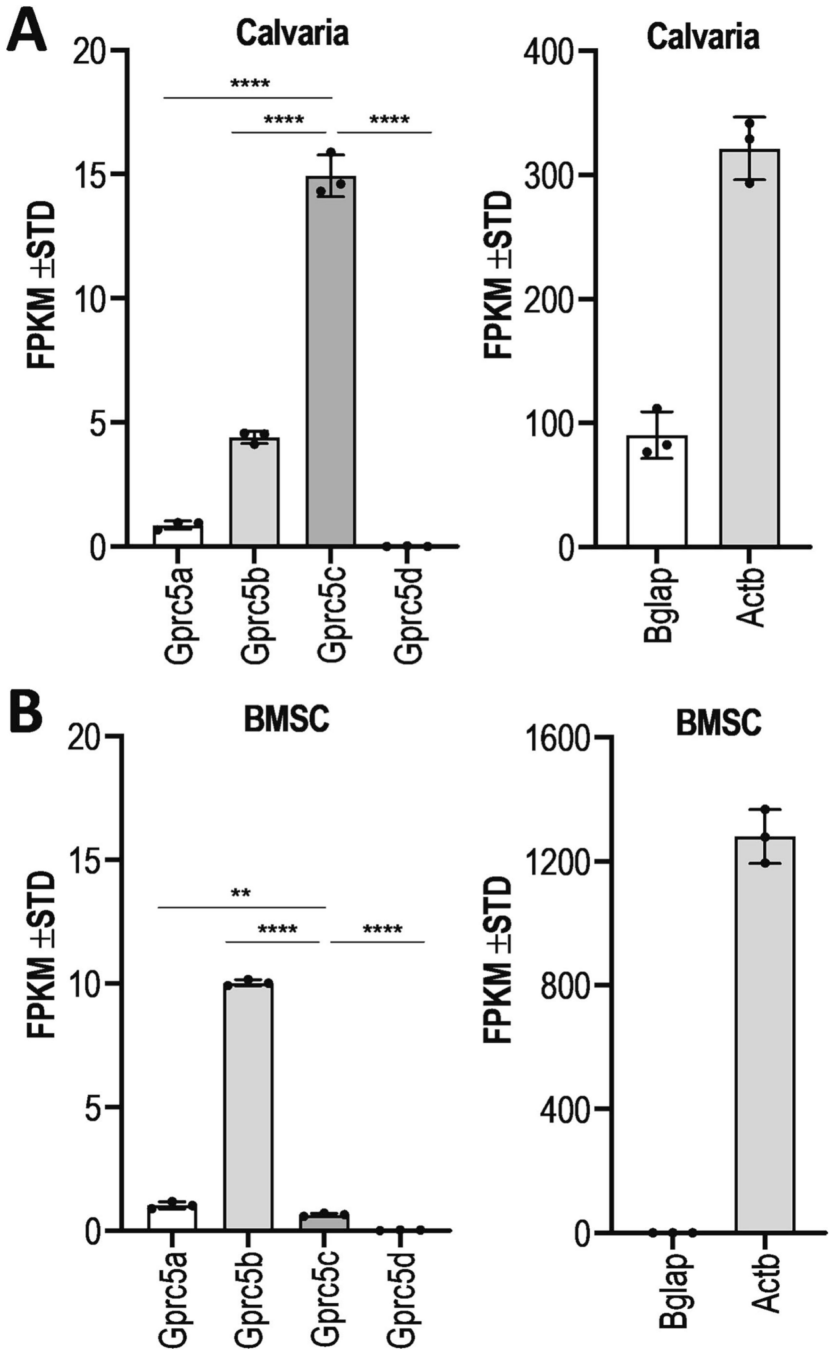

Figure 4: In vivo expression of Gprc5c mRNA in mouse calvaria and BMSCs.

RNA-seq data for Gprc5 mRNAs show that **(A)** Gprc5c is the most highly expressed member of the Gprc5 subfamily in Bglap positive mouse calvarial bone and that **(B)** Gprc5c is barely expressed in Bglap negative mouse bone marrow-derived mesenchymal stem cells (BMSC). Graphs show RNA-Seq expression for calvaria from three mouse pups (n = 3, mean ± STD); the bulk RNA-seq data were previously presented [44]; BMSCs were cultured under maintenance conditions [64]. Expression of Actb mRNA is shown for reference.

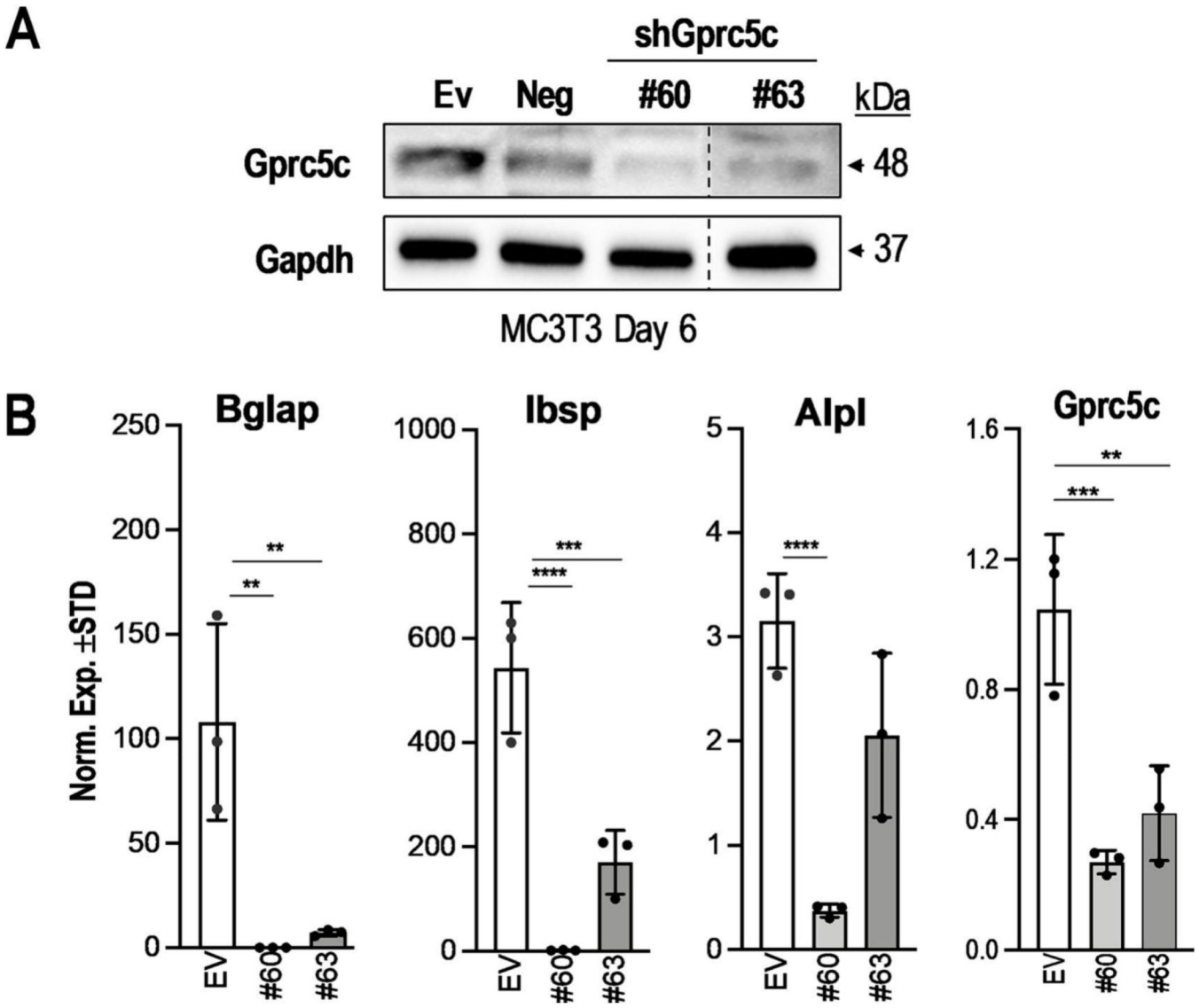

Figure 5: Gprc5c loss inhibits osteogenic differentiation of MC3T3-E1 cells.

Control and Gprc5c-depleted MC3T3-E1 cells were differentiated into osteoblasts (EV = empty vector; Neg = scrambled shRNA, #60 and #63 = Gprc5c targeting shRNAs). **(A)** Western blot analysis for Gprc5c and Gapdh on day 6 of differentiation. The dotted line in western blots indicate cuts in membrane that remove lanes that separate bands of interest. (**B**) RT-qPCR analysis for osteogenic mRNA markers (Bglap, Ibsp, and Alpl) and Gprc5c on day 6 of differentiation (n = 3, mean ± STD; ** = $p < 0.01$, *** = $p < 0.001$, and **** = $p < 0.0001$).

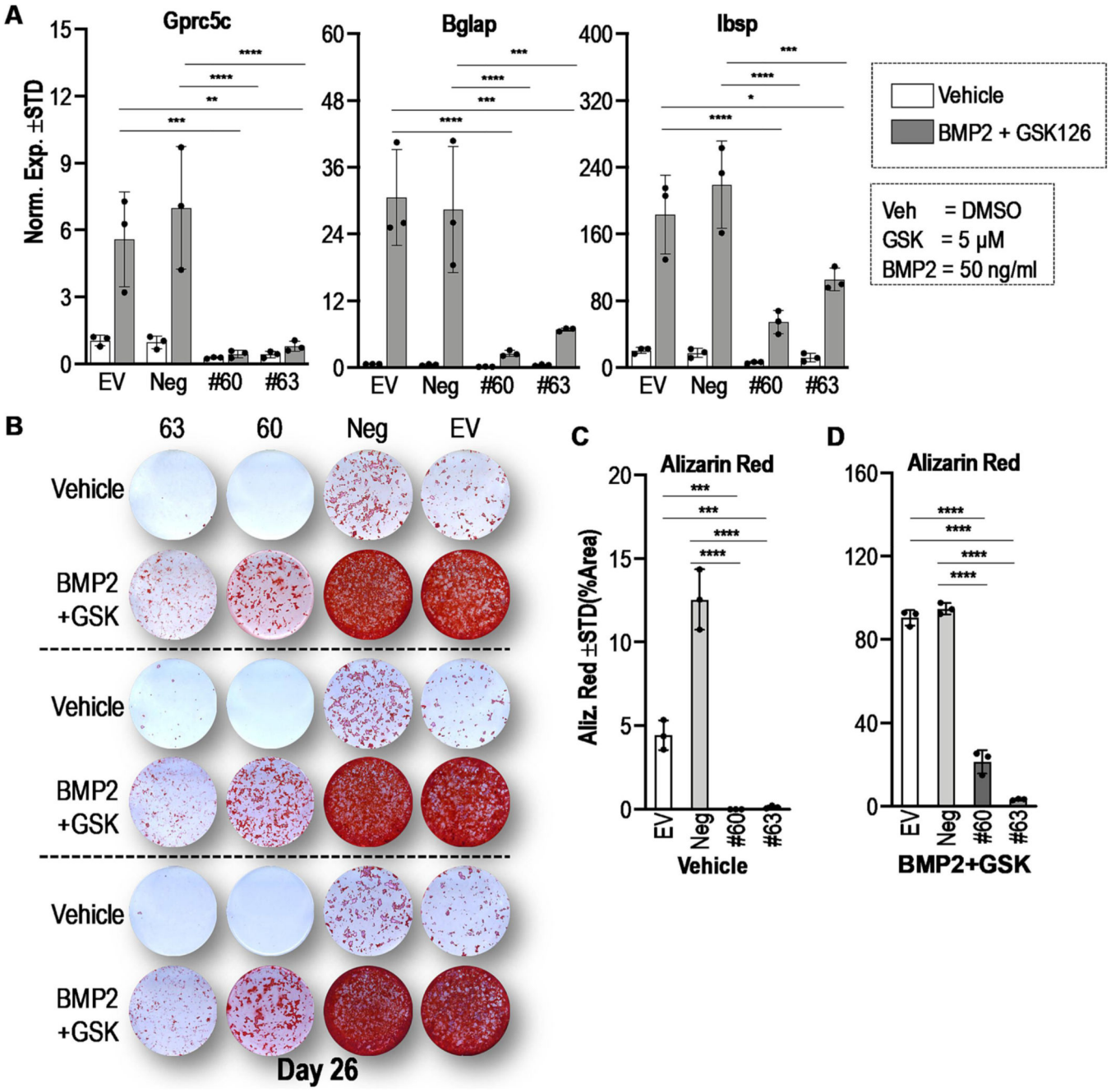

Figure 6: Gprc5c depletion impedes pro-osteogenic effects of BMP2 and GSK126 combination in MC3T3-E1 cells.

Control and Gprc5c-depleted MC3T3-E1 cells were differentiated into osteoblasts (EV = empty vector; #60 and #63 = Gprc5c targeting shRNAs) in the presence or absence of GSK126 (5 μM) and BMP2 (50 ng/ml). **(A)** RT-qPCR analysis was performed for Gprc5c and the osteoblast markers Bglap and Ibsp on day 6 of differentiation. **(B)** Representative examples of Alizarin Red staining in biological triplicates on day 26 differentiation. (**C&D**) Quantification of Alizarin Red staining was performed using Image J software. Statistical

significance was determined by two-way ANOVA (n = 3, mean ± STD; * = $p < 0.05$, ** = $p < 0.01$, *** = $p < 0.001$, and **** = $p < 0.0001$).

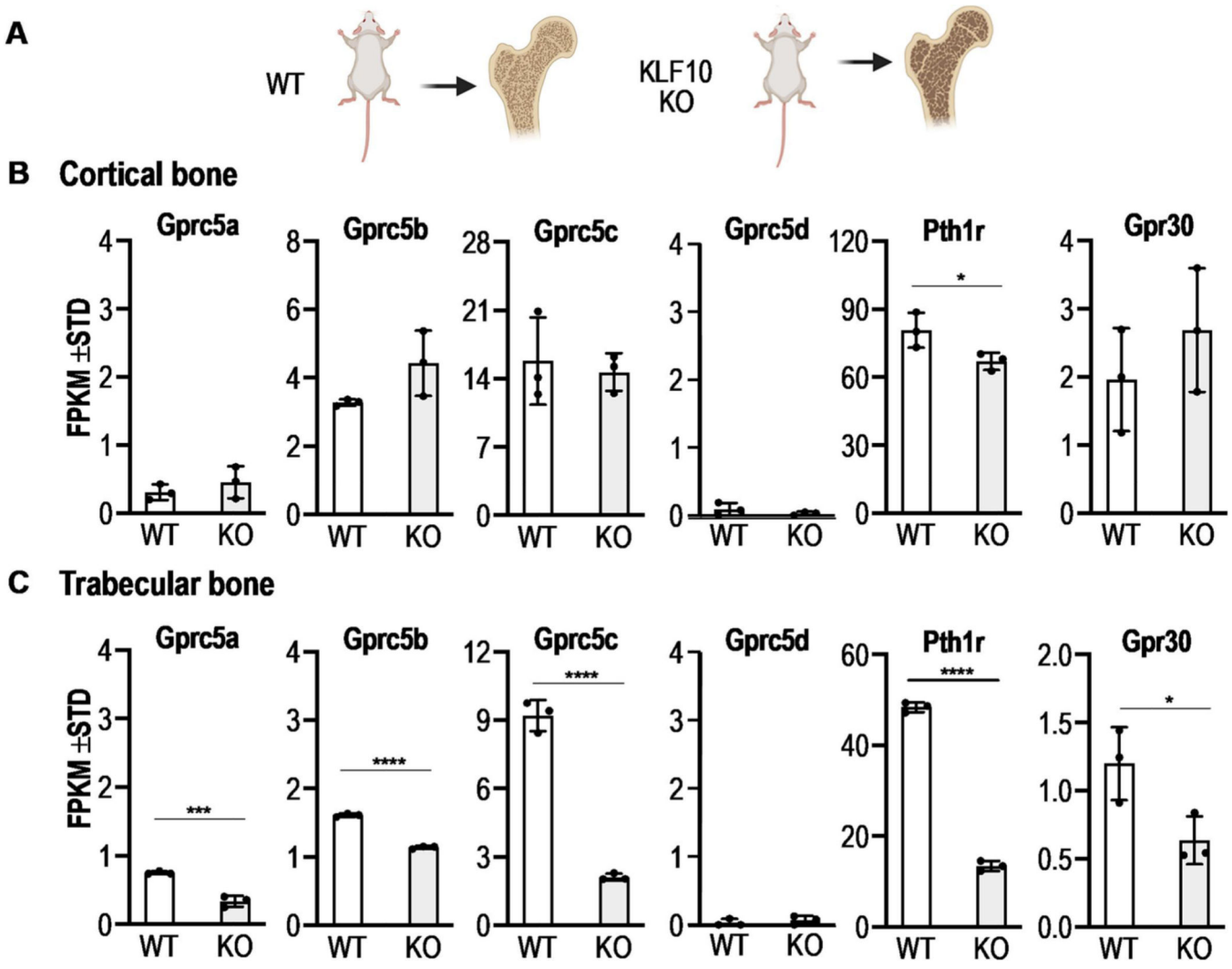

Figure 7: Gprc5c is suppressed in trabecular bone of an osteopenic Klf10 null mouse model.

Schematic illustration of Klf10 knockout osteopenic mice (**A**). RNA-seq analysis of female Klf10 knockout mice (n=3 biological replicates) for Gprc5 as well as Gpr30 and Pth1r mRNAs in **(B)** cortical versus **(C)** trabecular bone indicates that Gprc5c is selectively downregulated in Klf10 null mice compared to wild type in trabecular bone, but this reduction is not detected in cortical bone. Statistical significance was determined by two-way ANOVA (n = 3, mean ± STD; * = $p < 0.05$, ** = $p < 0.01$, *** = $p < 0.001$, and **** = $p < 0.0001$).

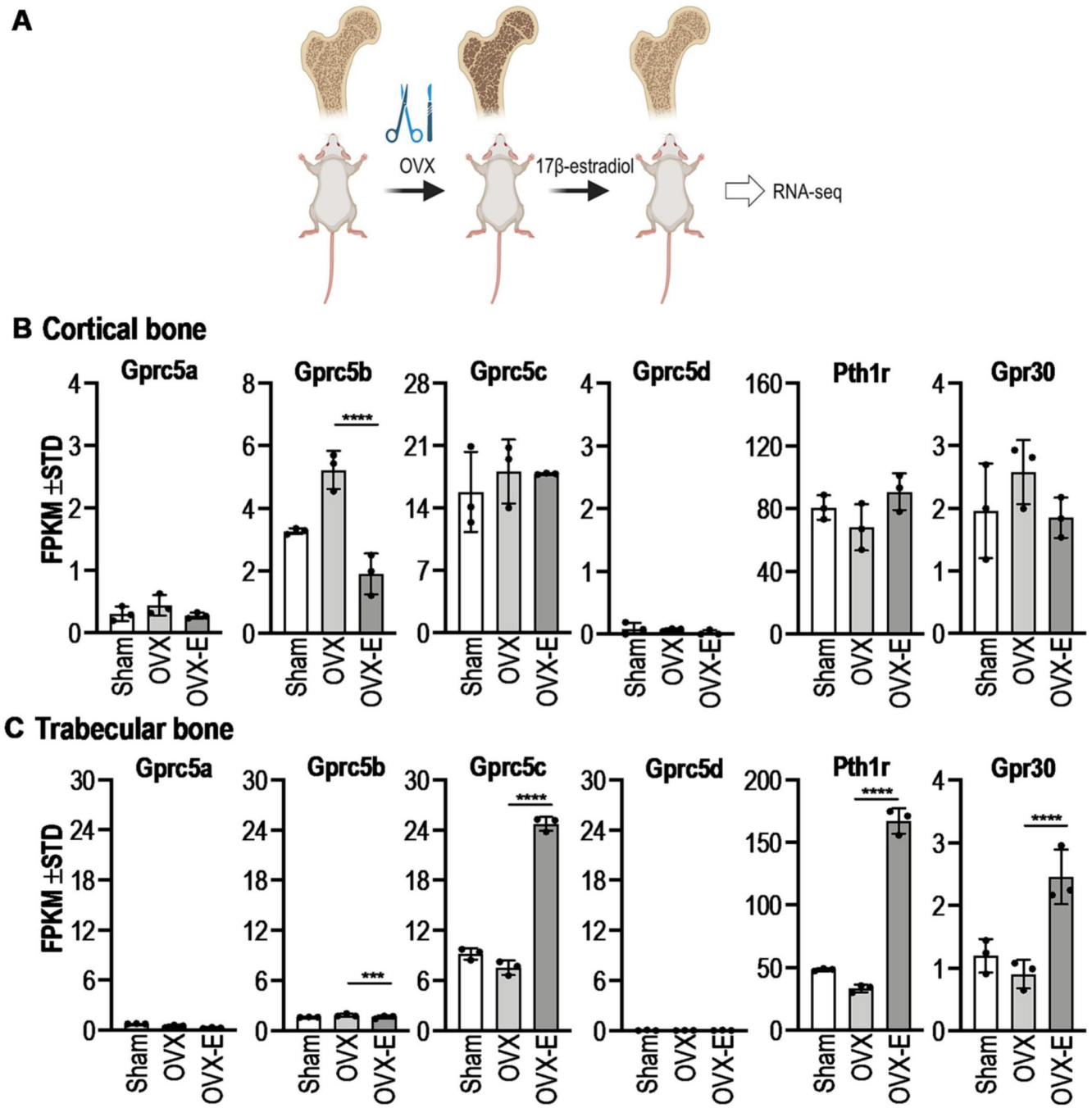

Figure 8: Gprc5c is induced upon 17β-estradiol administration in ovariectomized mice.

RNA-seq data from sham control and ovariectomized (OVX) mice versus OVX mice treated with estrogen (17β-estradiol) were used to assess Gprc5 as well as Gpr30 and Pth1r mRNAs in **(B)** cortical versus **(C)** trabecular bone. Statistical significance was determined by two-way ANOVA (n = 3, mean ± STD; * = $p < 0.05$, ** = $p < 0.01$, *** = $p < 0.001$, and **** = $p < 0.0001$). Gprc5c, Pth1r and Gpr30 are stimulated in parallel by estrogen supplementation in trabecular bone (**B**) and not in cortical bone (**C**).